2020 17th International Conference on Electrical Engineering, Computing Science and Automatic Control (CCE)
Mexico City, Mexico. November 11-13, 2020

Feasibility of Producing Acoustic Frozen Waves with Limited Number of Rings

A. Rodríguez-Peña[1], A. Vera[2], L. Leija[2], J. Gutierrez[3], J. Pérez-Orive[4], M.I. Gutierrez[5]*
[1]Instituto Nacional de Rehabilitación LGII – UNAM, DIIM, Mexico City, Mexico
[2]CINVESTAV-IPN, Department of Electrical Engineering, Bioelectronics, Mexico City, Mexico
[3]Instituto Nacional de Rehabilitación LGII, DIIM, Mexico City, Mexico
[4]Instituto Nacional de Rehabilitación LGII, Dirección de Investigación, Mexico City, Mexico
[5]CONACYT – Instituto Nacional de Rehabilitación LGII, SIB, DIIM, Mexico City, Mexico
*Email: m.ibrahin.gutierrez@gmail.com

Abstract — **In optics and acoustics, a particular solution of the wave equation, created by the superposition of Bessel beams of the same frequency, permits obtaining a stationary wave field with a static envelope in space. These solutions are called Frozen Waves and could have multiple potential applications. In this paper, the analysis of frozen waves using different levels of discretized finite aperture annular radiators is presented. The produced fields with these discretized radiators are compared with the field produced by a continuous finite aperture with the same radial distribution calculated to produce a single focus. The discretized radiator was based on a Bessel transducer varying the number of rings for each studied condition. Even though the acoustic frozen field is improved for the most numbers of rings (50 rings transducer), results with the 20 rings transducer show a similar pressure pattern at the focus. This would facilitate experiments for our future applications in ophthalmic ultrasound therapy.**

Keywords — **Frozen Waves, Kerf, Parametrization, Acoustic pressure.**

I. Introduction

The nondiffracting waves called Frozen Waves (FW) were first studied in optics, where different investigations established their main properties, such as stationary wave field, large depth of field and static envelope in space [1]. Such special solutions of the wave equation were first obtained theoretically in optics when using superimposed Bessel beams to produce a static and previously planned radiation pattern [1]–[3]. Ring based radiators have been proposed to produce the Bessel beams, and artificial "off-line" superpositions have been required to produce the resulted "Frozen" field [4]. Recent works have been proposing ways of combining the individual Bessel beams required to generate the prospected field pattern into just one field and be able to obtain experimentally the desired Frozen optical profile [5]. Applications in optical tweezers for small particle manipulation have been proposed using FW [3], [6].

After those initial works, some groups have extended the application of the FW to Acoustics, but still without concrete practical examples [7]. In this paper, an analysis of producing controlled acoustic radiation patterns with FW using a Bessel-ring finite aperture with a limited number of rings is presented. The distance between rings, named *kerf*, was kept constant [8], varying only the quantity of rings for radiating the field. A comparison is made versus the ideal situation when using a continuous finite radiator. The final intended application of this radiator is for ophthalmic ultrasound therapy in which we would reach the retina without damaging the most external tissues.

II. Methodology

A. Theory

Based on Dartora et al. [5], being $F(z)$ the desired longitudinal pattern for $r=0$ and $F(z)=0$ for $r\neq 0$, the radiation function for $z=0$ can be found by

$$p(r)=\int_{-\beta_{\max}}^{\beta_{\max}} F(\beta)\, J_0(\alpha r)\, d\beta, \qquad (1)$$

where $\alpha=\sqrt{k^2-(Q+\beta)^2}$, β is a variable coming from the transformation $k=Q+\beta$, Q is a positive constant in the range of $0.5k<Q<k$ restricted for forward propagation, and $F(\beta)$ is an adequate spectral function that can be determined based on the desired longitudinal pattern according to

$$F(\beta)=\frac{1}{2\pi}\int_{-\infty}^{\infty} F(z)e^{-j\beta z}d\beta; \qquad (2)$$

equation (2) is clearly showing a Fourier transform.

The amplitude and phase of the radiating pressure profile at the transducer surface can be obtained from the desired acoustic distribution substituting Eq. (2) into Eq. (1). For this paper, we were comparing the ideal continuous radiation with the discretization using a small number of rings. In this calculation, the chosen constants for the above equations in the interval $0<z<0.1$ m were given by

$$Q=0.99\cdot k$$

978-1-7281-8987-1/20/$31.00 ©2020 IEEE

$$\beta_{\max} = k - Q$$

k = wavenumber.

The obtained pressure of Eq. (1) is the solution for continuous cases limited only by the resolution of the acoustic field calculation and the discrete cases (concatenated arrangement of rings) that will be used to model the FW for discretized cases [5]. The desired longitudinal profile was given by

$$F(z) = u(z - Z_{p1}) - u(z - Z_{p2}) \qquad (3)$$

where u is the Heaviside step function, Z_{p1} and Z_{p2} are configurable depth-shift constants (time-shift of the real function).

The frozen waves were generated by integrating the difference of the Fourier transforms of two step signals, both signals depth-shifted at different points, to thereby obtain a configurable focus. The depth-shift of the signals is defined by the values Z_p previously selected for each of the two signals. The conditions for these shifts are given by

$$Z_{p1} < Z_{p2} \qquad (4)$$

$$Z_{p2} - Z_{p1} \approx \frac{L}{2}, \qquad (5)$$

where L is the maximum z-length on the field in which the frozen waves remain static [5]. For the models and graphs presented in this study, $L = 10$ cm, $Z_{p1} = 4$ cm and $Z_{p2} = 6$ cm ; these parameters were set with the objective to obtain a focal acoustic pressure preferably at the center of our model, with a shape of a square from 4 cm to 6 cm. The final application of this field is not discussed in this paper, since it only has the purpose of study the effect of the number of rings in the result with this kind of transducer.

B. Modeling setup

The simulations were carried out using the finite element method (FEM) with COMSOL Multiphysics 5.3 (COMSOL AB., Sweden) in a workstation 64 GB-RAM, 8 core-3.0 GHz microprocessor (Dell, USA). The pressure distribution was determined in water assuming the geometry is 2D axisymmetric and by solving the harmonic wave equation for lossless media given by

$$\nabla^2 p + k^2 p = 0. \qquad (6)$$

The solution was found for 3 MHz harmonic frequency using a triangular mesh of size $\frac{1}{3}\lambda$ resulting in 196,000 elements. Solution time using this configuration was about 10 s. Data were exported to MATLAB (MathWorks, USA) for postprocessing and graphing. After studying the radiation field in water, we could adapt the procedure to other water-based media as ocular tissues.

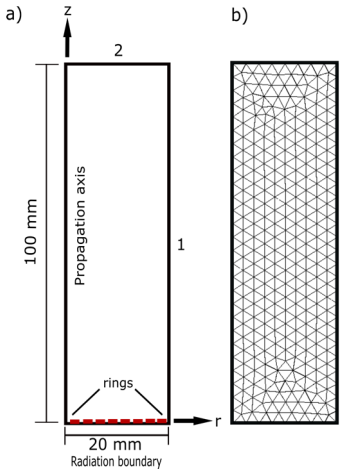

Fig. 1. (a) FEM geometry. (b) representation of the triangular mesh used (not showing the actual size).

The FEM geometry is shown in Fig. 1 which was designed to have the maximum length L and enough width to have a reduced reflection at boundary 1. Boundaries 1 and 2 were set with an acoustic impedance condition like that of water (propagating medium), which would help to reduce the ultrasound reflection at those boundaries. The ultrasound radiation was set at the bottom part of the geometry using two different approaches. The first one using a single boundary of 20 mm with the defined radiation of Eq. (1), with a radial resolution limited by the mesh size. The result of this approach was called "continuous" and was used as the "ideal" result for comparing the discretized approaches to be explained later. The second approach was carried out using a boundary discretization with an annular Bessel distribution [8].

C. Transducer annular discretization

The application of FW requires more realistic situations to be capable of producing the required distribution with a real transducer. A practical transducer capable of being driven with a controllable radiation pattern adaptable to the calculated required beam of Eq. (1) would require a level of discretization. Considering the FW are products of the superposition of Bessel beams, this discretization was made based on a Bessel annular transducer with a limited number of rings. The quantity of these rings was varied but keeping *kerf* constant at 10 μm, and their result were compared with the continuous radiation. It is expected that a transducer with

a very large number of rings would produce a better profile of FW; however, the challenge is to find an acceptable result with a small number of rings to be able to reduce the required practical amplifiers.

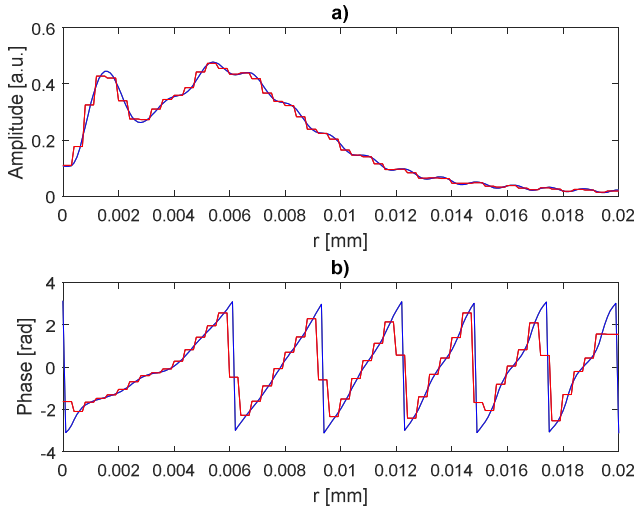

Fig. 2. Graph of the amplitude (a) and phase (b) of radiating pressure. *Blue*, continuous radiation; *red*, discretized for 50 rings.

Discretization of radiation function of Eq. (1) was carried out by averaging the data at different radial ranges controlled by the length of Bessel rings. Four different emissions were calculated for different quantity of rings: 10, 20, 40 and 50; the field of the transducer with 30 rings was also calculated but omitted in this paper for clarity, because its field did not significantly vary from that of 20 rings transducer. These levels of discretization corresponded to four different Bessel radiators [9]. The radial range between zeros of the Bessel function corresponded to a radial length of a ring. Figure 2 is showing a characteristic discretization with 50 rings of the amplitude and phase of an emitted radial profile determined with Eq. (1).

III. Results and Discussion

The simulations were made according to the conditions explained above. The most representative results are shown in Fig. 3 (results with 10 rings, 20 rings and 50 rings). The results of 40 rings are not shown because, in this kind of 2D representation, the acoustic field is very similar to each other and a more noticeable difference is more clear between the acoustic fields of 20 and 50 rings, especially on deeper areas; more discussion can be made at those different situations. The ideal case of Fig. 3a, when using a continuous radiator, shows how the field is concentrated at the expected zone (between 40 and 60 mm) with a very important reduction at other regions of the field. However, some extra waves were formed around the focus that could be the product of residual field that was not completely suppressed by the destructive interference. This could be due to the frequency used for the simulations, which could not be large enough to make some regions smoother.

The results with the discretized radiator using a finite number of rings are shown in Fig 3b to 3d for the cases with 10, 20 and 50 rings, respectively. Comparing the continuous case with these three figures, the best result was obviously the one using the greater number of rings, i.e. 50 rings. When using 10 rings, the field is very chaotic with too much energy out of focus. The pre-focal field is large, and the focus is not well defined. The result with 20 rings is comparable to that of 50 rings with just little improvement of the former at deeper regions, but not too much difference in the pre-focal zone. When using 50 rings, some important hot-spots appear in the pre-focal zone on the propagation axis ($r = 0$).

Some of these aspects can be more noticeable in the plots of Fig. 4. The acoustic pressure of these graphs was

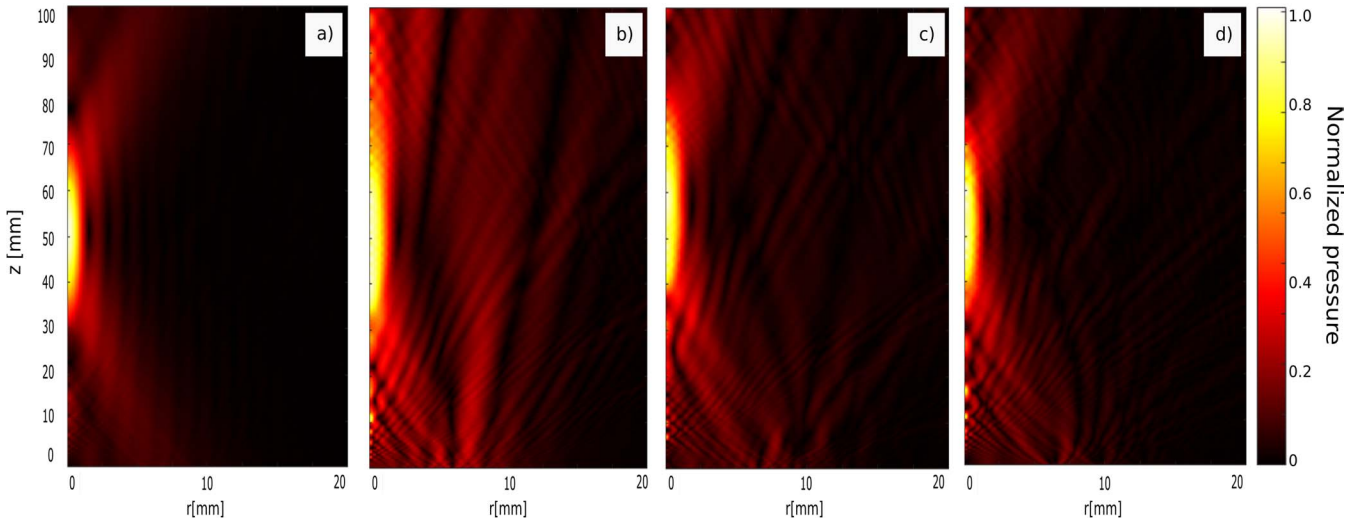

Fig. 3. Modeled acoustic field for the continuous radial distribution (a); discretization using 10 rings (b); 20 rings (c); and 50 rings (d).

normalized vs. the continuous result, assuming the discretization at the emitting boundary should produce the same average acoustic intensity at the source. From these graphs, we can see an improvement at the focus when using more rings started with 20, with minor variations in the pre-focal zone. The position of the focus was displaced from the continuous case, showing an improvement when a greater number of rings was used. As explained before, the result when using 50 rings produced some undesired hot-spots in the pre-focal zone not present in other graphs. The reasons of this could be coincidental since they could be product of some resonances at that specific combination of pressure, geometry, mesh, etc. and they may not be necessarily present in experimental radiators. However, this will be validated experimentally in the near future by our group.

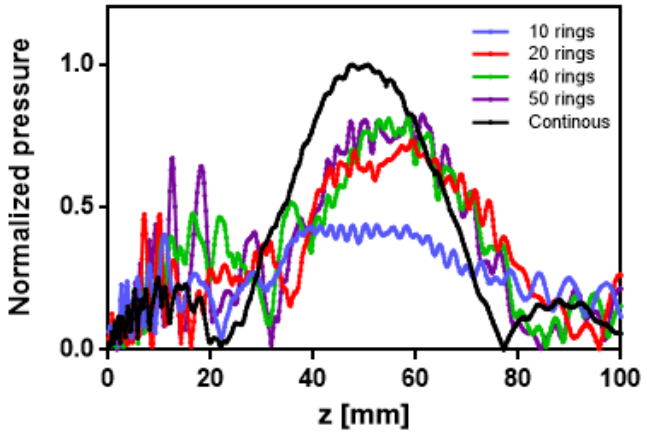

Fig. 4. Graph of the normalized acoustic pressures with different ring arrangements vs. the continuous radiation. Using discretized radiation produced larger pre-focal lobes than those in the ideal case. Using more than 20 rings did not significantly improve the results for this simulation.

IV. Conclusion

In the different simulations performed, comparing the baseline with the others, we observed significant changes that approach the continuous reference signal. Multiple variations are caused mainly by parameters like the width of the *kerf* and the total number of rings.

There is a tendency for the variations of the field to approach the result with the continuous signal for a larger number of rings, excepting at the pre-focal zone where the field distribution did not follow a predictive behavior. However, other parameters should be adjusted accordingly to obtain a more accurate result as the frequency, and the constants of the presented equations. Although theoretically there is no limit for choosing a very large number of rings for the radiator, in practice the required instruments should be considered, as the effect of a reduced *kerf*; increasing the number of rings implies having thinner rings, in which the ratio between the size of the ring and the size of the *kerf* would be smaller. The effect of this reduction should be also analyzed.

Acknowledgment

Authors would like to thank funding support by CONACyT CB2015-257966, ERAnet-EMHE 200022, CYTED-DITECROD-218RT0545, and Proyecto IV-8 call AMEXCID-AUCI 2018-2020. A. Rodríguez would like to thank CONACyT for undergrad thesis scholarship 29586.

References

[1] M. Zamboni-Rached, "Stationary optical wave fields with arbitrary longitudinal shape by superposing equal frequency Bessel beams: Frozen Waves," *Opt. Express*, vol. 12, no. 17, p. 4001, Aug. 2004.

[2] T. A. Vieira, M. R. R. Gesualdi, and M. Zamboni-Rached, "Frozen waves: experimental generation," *Opt. Lett.*, vol. 37, no. 11, p. 2034, Jun. 2012.

[3] T. A. Vieira, M. R. R. Gesualdi, M. Zamboni-Rached, and E. Recami, "Production of dynamic frozen waves: controlling shape, location (and speed) of diffraction-resistant beams," *Opt. Lett.*, vol. 40, no. 24, p. 5834, 2015.

[4] J. L. Prego-Borges, M. Zamboni-Rached, E. Recami, and H. E. Hernández-Figueroa, "Producing acoustic frozen waves: Simulated experiments," *IEEE Trans. Ultrason. Ferroelectr. Freq. Control*, vol. 60, no. 11, pp. 2414–2425, 2013.

[5] C. A. Dartora, K. Z. Nobrega, A. Dartora, G. A. Viana, and H. S. Filho, "A general theory for the Frozen Waves and their realization through finite apertures," *Opt. Commun.*, vol. 265, no. 2, pp. 481–487, Sep. 2006.

[6] M. Corato-Zanarella and M. Zamboni-Rached, "Electromagnetic frozen waves with radial, azimuthal, linear, circular, and elliptical polarizations," *Phys. Rev. A*, vol. 94, no. 5, pp. 1–9, 2016.

[7] J. L. Prego-Borges, M. Zamboni-Rached, E. Recami, and E. T. Costa, "Producing acoustic 'Frozen Waves': Simulated experiments with diffraction/attenuation resistant beams in lossy media," *Ultrasonics*, vol. 54, no. 6, pp. 1620–1630, 2014.

[8] L. Castellanos, I. Bazan, and A. Ramirez-Garcia, "A transducer array design for acoustic frozen waves generation with a kerf optimization for biomedical applications," *Pan Am. Heal. Care Exch. PAHCE*, no. 4, pp. 1–4, 2014.

[9] M. I. Gutierrez, H. Calas, A. Ramos, A. Vera, and L. Leija, "Acoustic Field Modeling for Physiotherapy Ultrasound Applicators by Using Approximated Functions of Measured Non-Uniform Radiation Distributions," *Ultrasonics*, vol. 52, no. 6, pp. 767–777, 2012.